Research Square

Preprints are preliminary reports that have not undergone peer review.
They should not be considered conclusive, used to inform clinical practice,
or referenced by the media as validated information.

Sustainable Production of Magnetic Activated Carbon from Agricultural Waste for the Adsorption of Cationic and Anionic Dye in Single, Binary and Ternary System

A Shehu

akchemist88@gmail.com

Bayero University Kano (BUK)

Muhammad A. S

Bayero University Kano (BUK)

Ibrahim M. A

Bayero University Kano (BUK)

Abdulganiyu R. A

Federal College of Agricultural Produce Technology

Research Article

Keywords: Adsorption, Kinetic, Equilibrium, Co-adsorption, Magnetic and Activated Carbon

Posted Date: November 10th, 2026

DOI: https://doi.org/10.21203/rs.3.rs-11441981/v1

License: This work is licensed under a Creative Commons Attribution 4.0 International License.
Read Full License

Additional Declarations: No competing interests reported.

Sustainable Production of Magnetic Activated Carbon from Agricultural Waste for the Adsorption of Cationic and Anionic Dye in Single, Binary and Ternary System

[1]Shehu A*, [2]Muhammad A.S, [3]Ibrahim M.A, and [2]Abdulganiyu R.A,

[1]Departments of General Studies, Federal College of Agricultural Produce Technology, P.M.B. 3013, Kano, Nigeria

[2]Department of Pure and Industrial Chemistry, Faculty of Physical Sciences College of Natural and Pharmaceutical Sciences, Bayero University Kano (BUK), P.M.B. 3011, Kano, Nigeria.

[3]Department of Applied Chemistry, Federal University of Technology, Babura, Jigawa State

*Corresponding author Email address: akchemist88@gmail.com

Abstract

The simultaneous removal of dyes from industrial wastewater remains a significant challenge, particularly because the mechanisms governing dye co-adsorption are not yet fully understood. In this study, magnetic activated carbon (MAC) was prepared through a simplified chemical modification process and employed as an adsorbent for the removal of malachite green (MG) in single- and multicomponent dye systems. The adsorption behaviour of MG in the presence of other dyes was investigated to evaluate the interactions and competitive effects during co-adsorption. The experimental results showed that the adsorption capacities in multicomponent systems were generally comparable to those observed in single-solute systems. The adsorption kinetics was best described by the pseudo-second-order model in both single and multicomponent systems, with coefficients of determination (R^2) approaching unity. Furthermore, the extended Langmuir model, freundlich and Dubinin Rdushkevich adequately described the equilibrium data for the co-adsorption process. The maximum adsorption capacities for MG, MG + BBE 133, MG + NR, and MG + NR + BBE 133 were 16.86, 23.31, 14.41, and 10.36 mg/g, respectively. The observed variations in adsorption capacity indicated the presence of both synergistic and antagonistic effects, depending on the dye combination, with antagonistic behaviour evident in the binary system containing MG and NR. The co-adsorption process was potentially governed by hydrogen bonding, π–π stacking interactions, and electrostatic interactions between the dyes and the MAC surface. Overall, the findings highlight the potential of MAC as an effective adsorbent for dye removal from aqueous solutions and provide insights into the interactions influencing dye adsorption in multicomponent systems.

Keywords: Adsorption, Kinetic, Equilibrium, Co-adsorption, Magnetic and Activated Carbon

1. Introduction

Due to its pollution and scarcity, the water crisis has generated widespread concern worldwide. Several complex contaminants from industrial and domestic activities are indirectly or directly released into water bodies (Patra *et al*., 2021). In this context, dyes are the main organic contaminants (Haleem *et al*., 2023). These compounds are widely used in textile, leather,

cosmetics, plastic, pharmaceutical, food processing, and other industrial sectors (Alia *et al*., 2019). Currently, more than 100,000 commercial dyes are available, and the estimated annual production of synthetic dyes is about 30,000 tons (Haleem *et al*., 2023). A large part of these dyes is usually discharged into water bodies through untreated wastewater either in single or multiple forms, a considerable pollution source (Shah *et al*., 2019). In general, dyes have a complex chemical construction, making their degradation difficult, and consequently they remain longer in the environment. The presence of dyes in water bodies can affect the photosynthetic activity of aquatic life (Bhatti *et al*., 2020; Wekoye *et al*., 2020). In addition, it can affect some conditions, such as biological and chemical oxygen demands, dissolved oxygen concentration, pH, and the life of aquatic animals and their predators. Thus, the treatment of wastewater containing dyes is a very relevant issue. Several technologies have been used to remove dyes from wastewater, such as advanced oxidation processes (Ortiz martinez *et al*., 2021), flocculation/coagulation (Dotto *et al*., 2018), biological treatments (Arunprasath *et al*., 2019), ion exchange (Hassan and Carr, 2018), and adsorption (Desalomon *et al*., 2020). Among these methods, adsorption is a promising technique for removing colored contaminants from wastewater (Dotto and Mackay, 2020). Adsorption is promising since it has advantages such as applicability in different scenarios, ease of implementation, low space requirement, design simplicity, economic feasibility, and high efficiency (Tahir *et al*., 2016; Jawad *et al*., 2020). In adsorption operations, activated carbon (AC) is widely used for removing inorganic and organic contaminants from aqueous solutions (Puchana *et al*., 2016; Yunus *et al*., 2020). This adsorbent presents high surface area, pore volume, and abundant surface functional groups (Rashid *et al*., 2019). In parallel, the utilization of lignocellulosic wastes as precursor materials for AC production is a viable alternative due to its low cost, availability, and ecological suitability (Kang *et al*., 2020; Sarkar *et al*., 2021; Supong *et al*., 2019). In previous literature, several studies have been carried out on developing AC from different lignocellulosic wastes such as pecan nutshells (Zazycki *et al*., 2018), tangerine seed (Wang *et al*., 2020), banana peel (Valhuan *et al*., 2017), apple peel (Enniya *et al*., 2018), pistachio wood wastes (Sajjadi *et al*., 2019), and teak wood sawdust (Kumar and Gupta, 2020). Specifically, *Anana comosus* peels (ACP), is a lignocellulosic waste, accessible, abundant, and low-cost by-product and presents disposal problems. Thus, the conversion of *Anana comosus* peels into adsorbents is a good alternative for managing this waste. In addition, the development of magnetic adsorbents has also been highlighted since it facilitates the separation of the solid from the liquid phase without requiring centrifugation (Veira *et al*., 2020; Liu *et al*., 2020; Moosevi *et al*., 2020; Wang *et al*., 2020). Therefore, magnetic-activated carbons (MAC) have recently been proposed to remove contaminants (Du *et al*., 2020; Feng *et al*., 2020; Pereira *et al*., 2020; Saleem *et al*., 2020). Generally, these magnetic-activated carbons are prepared by co-precipitation, the activated carbon's impregnation of the precursor material, followed by pyrolysis (Thur *et al*., 2020). In the last procedure, carbonization, activation, and magnetization occur in a single step an economic and convenient advantage (Bai *et al*., 2015). However, regardless of the preparation method, evaluating different experimental conditions to prepare AC is fundamental to finding a material

with relevant features for adsorption (Dotto and Mckay, 2020). Herein, MACs were produced from *Anana comosus* peels, characterized, and applied in dye adsorption from an aqueous solution. The precursor was first impregnated with KOH and HCl; then, the impregnated materials underwent pyrolysis. Characterization was performed by scanning electron microscopy (SEM), Fourier transform infrared spectroscopy (FTIR), Brunauer–Emmett–Teller (BET), X-ray diffraction (XRD). Adsorption studies involved kinetic and equilibrium experiment and test with simulated industrial effluents.

2 Materials and Method

2.1 Sample Collection and Preparation

Ananas Comosus peels (ACP) was collected from Yan Lemu Market, Kumbotso Local Government, Kano state, Nigeria. The sample was washed and dried at room temperature for 24 h to remove moisture. The dried samples were pulverized using pestle and mortar, and sieved to obtain particle size of 250 μm. 50 g of the sample was impregnated with 30 % KOH and aged for 24 h. The impregnated sample was then subjected to thermal activation muffle furnace at 450 °C for 3h. The activated sample was neutralized with 0.1M HCl, followed by washing with distilled water to remove the traces of undissolved chemicals. It was subsequently dried in an oven at 80 °C for 6 h to removed moisture content then stored for further application.

2.2 Preparation of Magnetic Activated Carbon

100 g of AC was suspended in three volumetric flasks containing 500 cm^3 of distilled water each. A ferric chloride solutions were freshly prepared by adding 18 g of $FeCl_3 \cdot 6H_2O$ to 1300 cm^3 of distilled water in three different volumetric flasks. A ferrous sulfate solutions were prepared by adding 20 g of $FeSO_4 \cdot 7H_2O$ to 150 cm^3 of distilled water in three different volumetric flasks. Each of the prepared solutions were mixed and vigorously stirred at 60–70°C. The mixture were added to an aqueous suspension of activated carbon at room temperature and slowly stirred for 30 minutes. After mixing, 10 M NaOH was added dropwise into the suspension until the pH rises to 10–11. The suspensions were aged at room temperature for 24 hours and then repeatedly washed with distilled water, followed by ethanol, and subsequently dried at 25 °C (Shehu and Muhammad, 2026).

2.3 Preparation of stock solution

1 g of the respective dye was dissolved in 1 liter distilled water, resulting in a concentration of 1000 mg/L. The binary and ternary dye solution, consisting of MG, NR and BBE133, was also prepared in the same manner, with a mass ratio of 1:1 or 1:1:1. From the stock solution,

experimental solutions of lower concentrations were subsequently generated through successive dilution. These solutions were used for constructing the calibration curve and conducting adsorption studies.

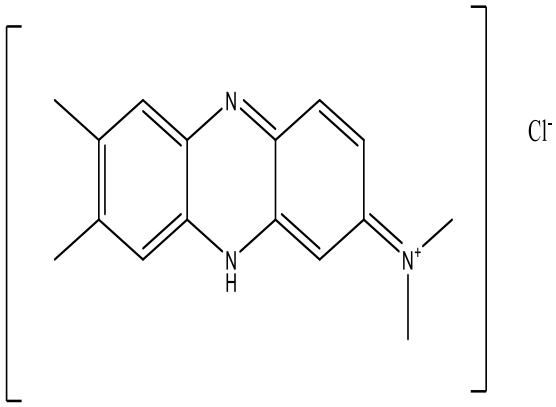


Fig.1 Structure of Neutral Red

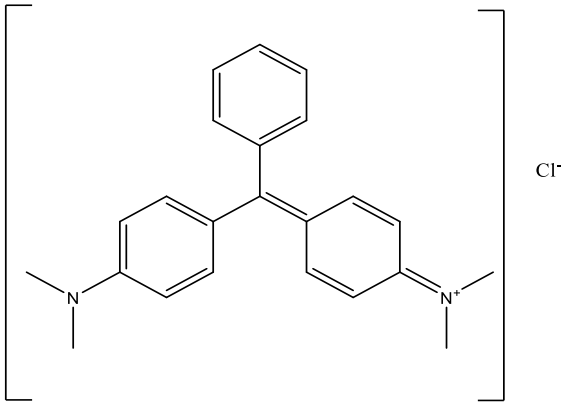


Fig. 2 Structure of Malachite Green

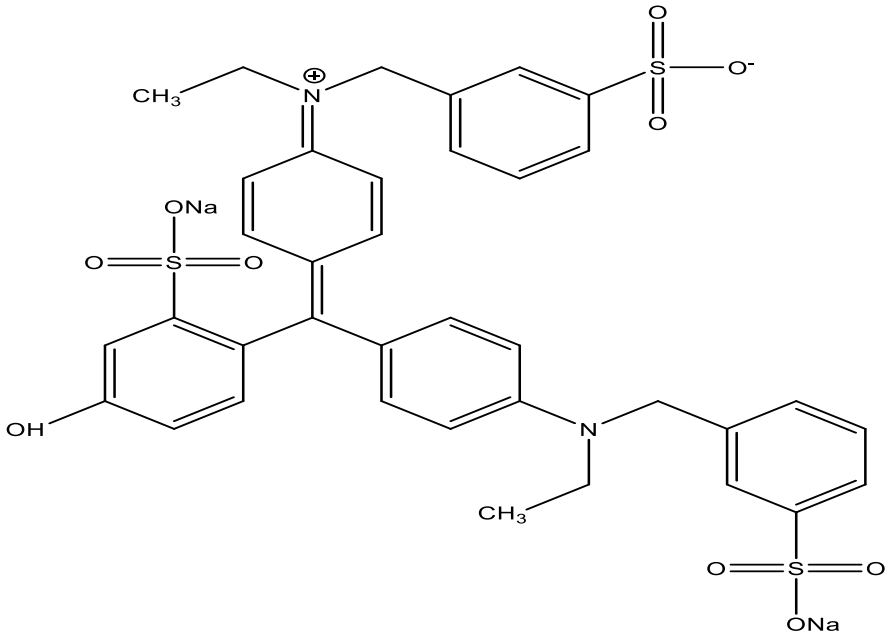


Fig. 3 Structure of Brilliant Blue E133

3. Results and Discussion

3.1 Fourier Transform Infrared (FTIR)

The FTIR spectra of ACP and ACPMAC are shown in Fig. 4a. it was observed the peaks at approximately 3400 cm^{-1} was attributed to –OH groups, while the band near 2900 cm^{-1} corresponded to $–CH_2$ stretching vibrations. The band observed around 1700 cm^{-1} was associated with C=C aromatic stretching, whereas the band at 1600 cm^{-1} was assigned to C=O stretching. Additionally, the absorption band near 1000 cm^{-1} was linked to C–O stretching. Following adsorption, shifts and broadening of these peaks were observed, indicating their involvement in the adsorption process. A new peak appearing at 700 cm^{-1} confirmed the presence of Fe–O stretching, which resulted from the loading of magnetic particles onto the adsorbent surface. Collectively, these findings suggest that while adsorption occurred, the overall structural integrity of the adsorbents remained intact, and the synthetic dyes were adsorbed without altering their fundamental chemical structures (Chen *et al*., 2020).

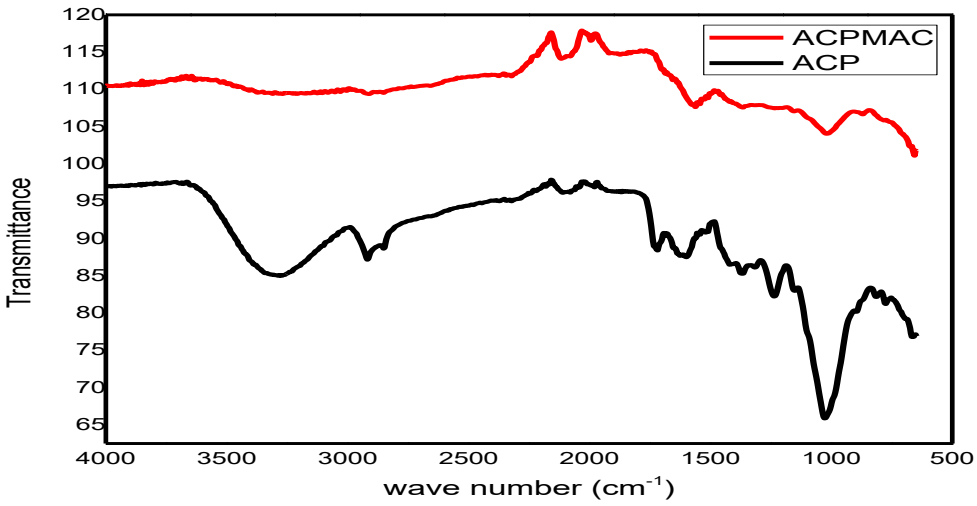


Fig. 4a: FTIR spectra for ACP and ACPMAC

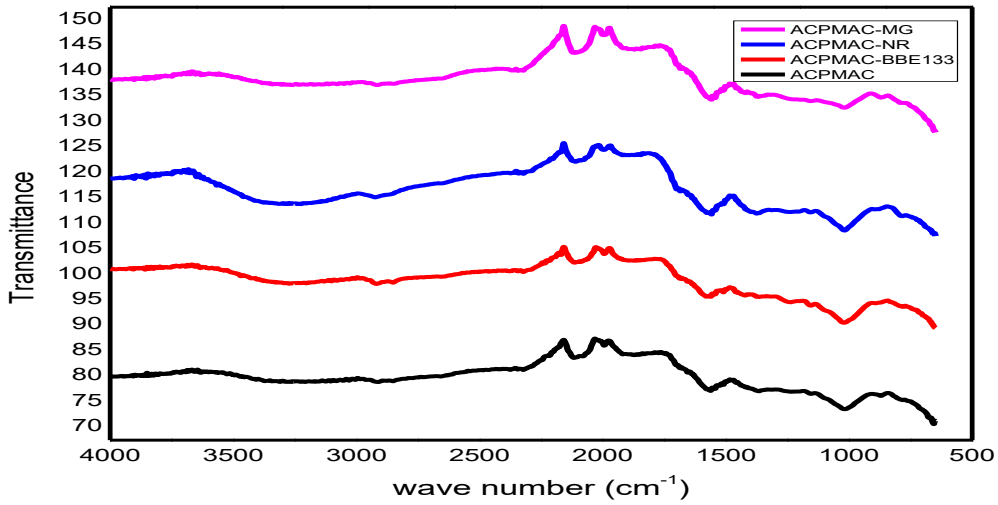


Fig. 4b: FTIR spectra for ACPMAC before and after adsorption

3.2 Scanning Electron Microscope (SEM)

The SEM micrograph of ACP is presented in Fig. 5a reveal non-porous and microporous surfaces devoid of cracks and cavities. Following magnetization, the surface morphology in Fig. 5b demonstrates increased roughness, with the presence of cracks and cavities. This transformation is attributed to the incorporation of magnetic particles, which enhanced the adsorbents' properties by generating a heterogeneous surface morphology characterized by disorganized structural patterns (Grabi *et al*., 2023). Such heterogeneity is advantageous for adsorption, as it provides multiple interaction sites for contaminants.

Fig. 4(c-e) indicated significant changes in surface morphology of ACPMAC before and after interaction with MG, NR and BBE133 dyes which appeared smoother, with scattered pores partially covered by adsorbate molecules. This observation suggests that the adsorbents possess excellent adsorption properties, and their modified structures facilitate enhanced dye uptake (Bai *et al*., 2020).

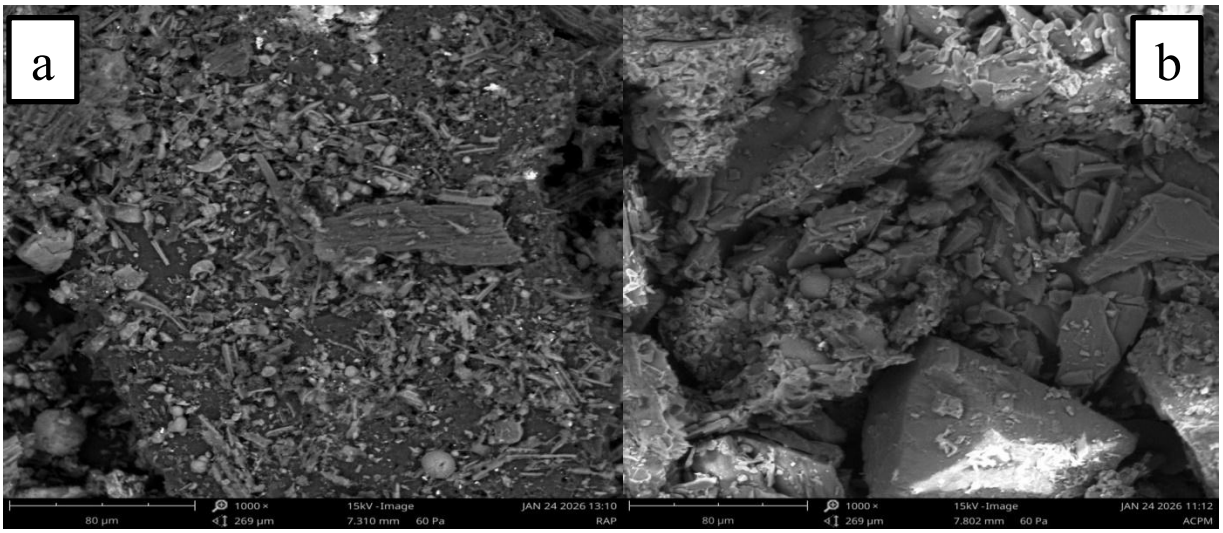


Fig. 5a SEM Micrographs of a) ACP b) ACPMAC

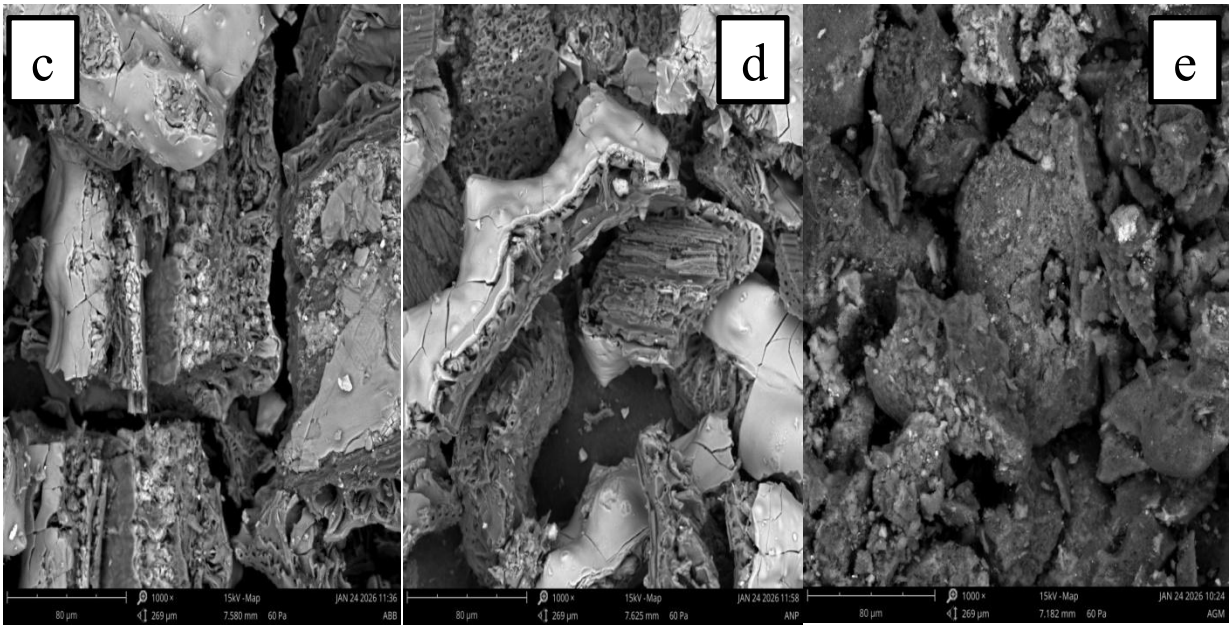


Fig. 5b SEM Micrographs of a) ACPMAC-BBE133 b) ACPMAC-NR c) ACPMAC-MG

3.3 X–ray Diffraction (XRD) Analysis

The XRD patterns of ACP and ACPMAC reveal differences in their structural characteristics following magnetic modification. ACP exhibit diffraction feature centered approximately 2θ=20–25 °C, indicating a predominantly amorphous or poorly crystalline carbon structure typical of biomass–derived activated carbon. In contrast, ACPMAC displays substantially higher diffraction intensity, suggesting an alteration in the diffraction response following the

incorporation of iron containing species. However, the characteristic diffraction peak of hematite are not clearly resolved in the presented pattern (Anyika *et al*., 2017: Reza and Ahmaruzzaman, 2015).

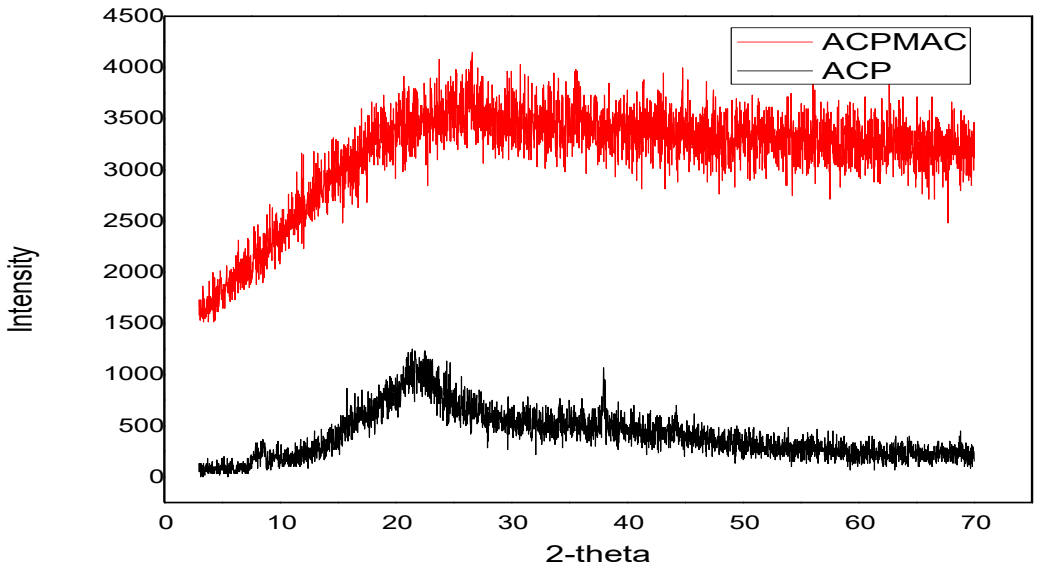


Fig. 6 X–ray Diffraction spectra

3.4 Brunauer Emmett Teller (BET) Surface Area Analysis

Nitrogen adsorption–desorption measurements were carried out at 77K to evaluate the textural properties of the synthesized ACPMAC samples. The obtained BET plot and Barrett–Joyner–Halenda (BJH) pore volume plot were shown in Fig. 6a while the Pore Distribution Plots were shown in Fig. 6c. The BET surface area were calculated using the multi-point BET method in the linear region of the BET plot, corresponding to a relative pressure (P/P_0) range of 0.049–0.303, following IUPAC guidelines for mesoporous and microporous solids (Thommes *et al.,* 2020).

The BET plots for each adsorbent displayed a well-defined linear region, and the linear regression analysis produced a slope of 5.003, Intercept of 6.025, correlation coefficient (R^2): 0.9912, BET constant (C) of 1.830, generating a BET surface area of 315.768 m^2/g for ACPMAC sample. The BET surface area and constant (C), suggested moderate adsorbate–adsorbent interactions, characteristic of materials with a mesoporous features while the linearity (R^2) confirms the suitability of the selected pressure range and validates the BET analysis.

Pore structural properties were evaluated using the Barrett–Joyner–Halenda (BJH) method based on the adsorption branch of the isotherm. The BJH method provides insights into mesopore distribution, pore size, and pore volume rather than true surface area. The BJH analysis based on the adsorption branch provides information on the mesopore structure of the ACPMAC. The BJH results for ACPMAC indicate a Cumulative mesopore surface estimate of 231.476 m^2/g, a Pore volume of 0.121 cm^3/g and average pore diameter (BJH Dv(d)) 2.137 nm. This implies that the materials exhibit mesoporosity, falling within the IUPAC-defined mesopore range of 2–50 nm. The pore diameter around 2 nm which suggests a predominantly mesoporous structure is highly favorable for adsorption of dye molecules. Similar textural properties have been reported for other biomass-derived magnetic activated carbons. *Sajab et al*., (2024) reported a magnetic activated carbon derived from *Artocarpus heterophyllus* peel with a surface area of 290.763 m^2/g, pore volume of 0.160 cm^3/g, and pore diameter of 2.80 nm. The closeness of these values indicates that the prepared adsorbent possesses textural properties comparable to other effective agricultural waste-based magnetic activated carbons reported in literature, confirming its potential suitability for adsorption applications. It should be noted that the BJH "surface area" is not a replacement for the BET area; instead, it measures the surface contribution of mesopores specifically.

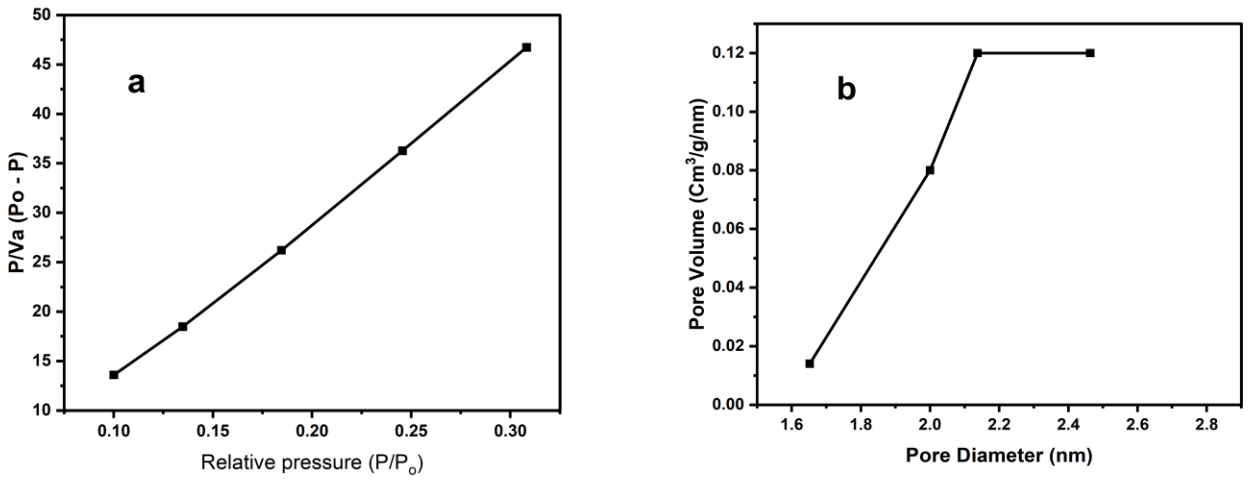


Fig. 6 (a) linear fitting of ACPMAC (b) ACPMAC Pore Volume Plot

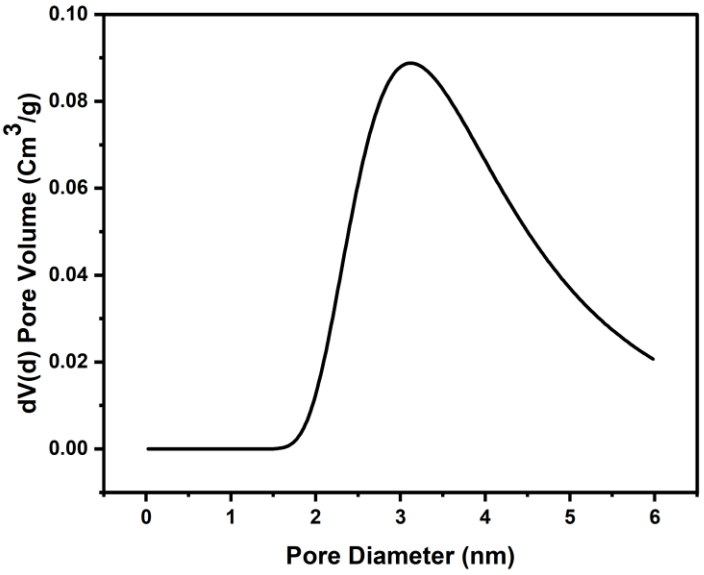


Fig. 6 Pore Distribution Plot of ACPMAC

3.5 BATCH ADSORPSION EXPERIMENT

3.5.1 Effect of Contact time:

It is essential to explore how quickly substances are adsorbed in the design adsorption process. Faster adsorption rates lead to lower operational costs, making the adsorbent more suitable for large-scale applications (Istratie *et al*., 2019). To determine the optimal time required to maximize the removal of dye molecules. Fig. 7 shows the MG adsorption in single, binary and ternary systems increased rapidly with the initial 15–30 minutes before reaching a relatively stable plateau. The minimal variations among the systems suggest similar adsorption behaviors under experimental conditions, although competitive interactions may occur in the multicomponent solutions (Noozi and Sorial, 2013).

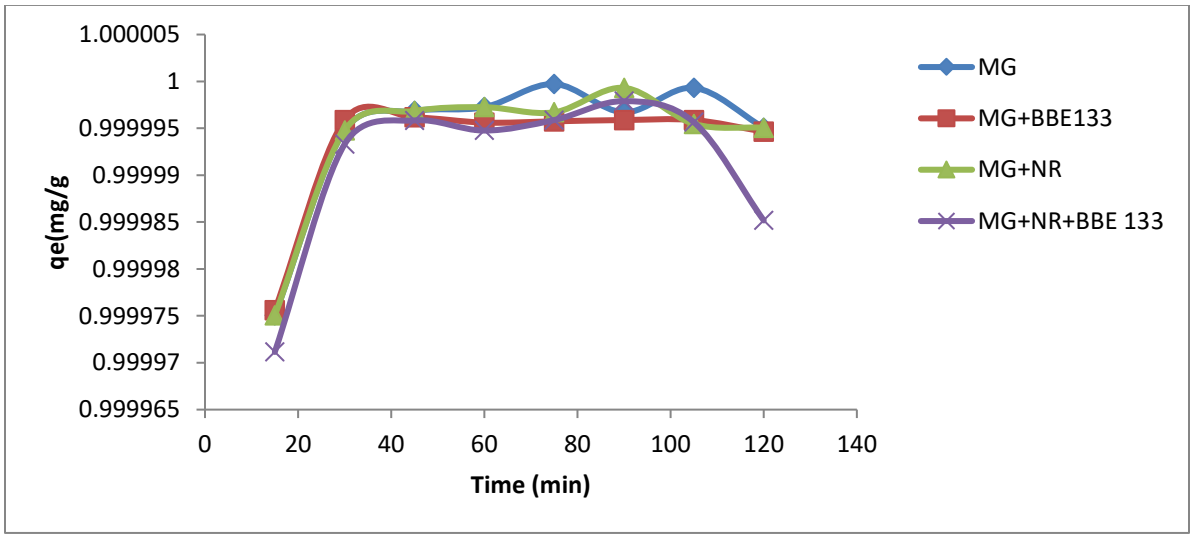


Fig. 7 Effect of Contact Time

3.5.2 Effect of dosage

The quantity of MG adsorbed per unit mass of adsorbent, indicated as qe, decreased as the adsorbent dosage increased across various adsorbate systems (single, binary, and ternary), as shown in Fig 8. With an increase in the adsorbent dose from 0.1 to 0.6 g, the adsorption capacity (qe) consistently decreased in all the adsorbates due to the interaction and aggregation of particles at higher dosage resulting in the reduction of surface area and active sites. This finding suggested that at lower doses, the active sites on the surface of the adsorbent were effectively

utilized, but with an increase in the adsorbent dosage, a significant portion of these active sites likely overlapped, resulting in a decrease in the specific uptake.

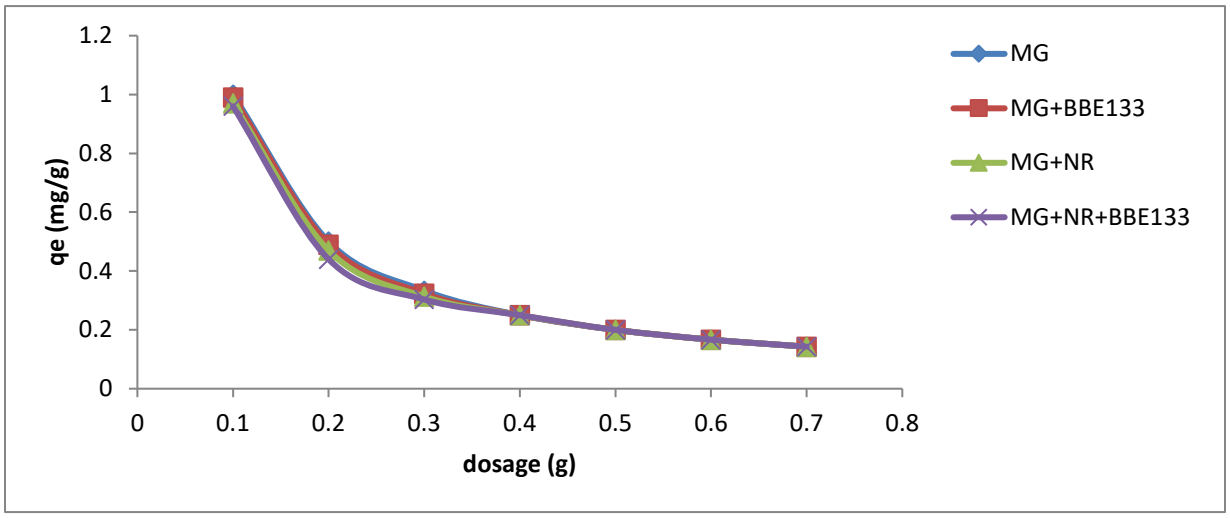


Fig. 8 Effect of Dosage

3.5.3 Influence of Initial Concentration

The initial concentration of the adsorbate plays a crucial role in determining the diffusion and mass transfer dynamics of dye sorption onto the adsorbent. Figure 4b illustrates the impact of the initial concentration on the removal efficiency of the adsorbates. Higher initial concentration provides the necessary driving force to overcome mass transfer resistance for the transport of dyes between the aqueous phase and the surface of adsorbent (Duran *et al*., 2011). As observed from the plot, the percentage of the dyes removed decreases due to the saturation point of the adsorbent that limit its capacity to adsorb more dye molecule, this results in lower percentage removal compared to the cases with lower initial concentrations (Husaini *et al*., 2024a).

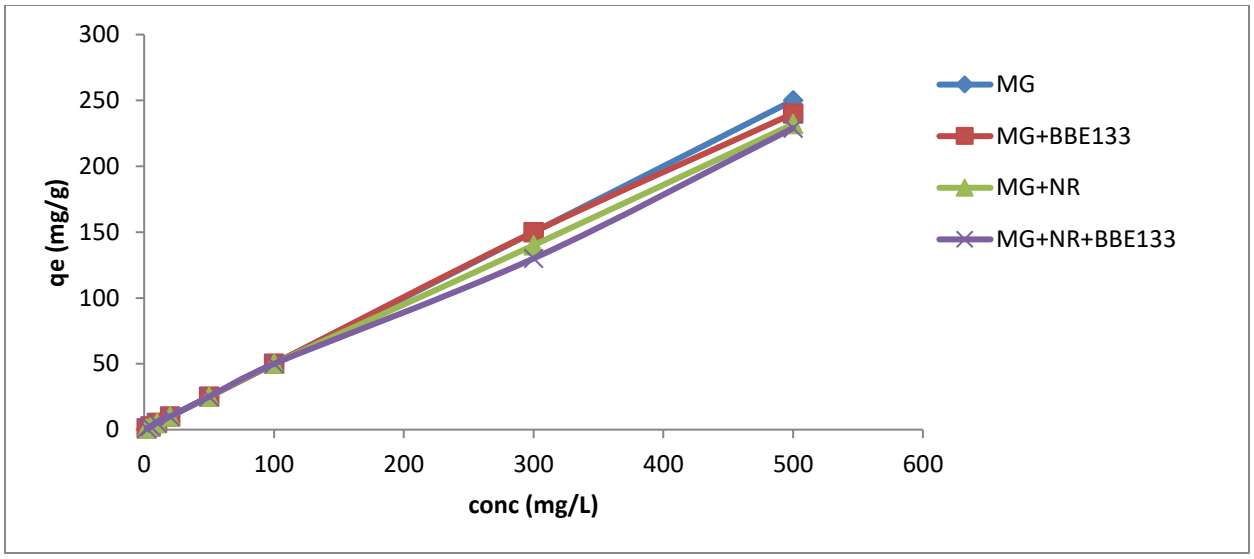


Fig. 9 Effect of Concentration

3.5.4 Effect of pH

Fig. 10 shows that pH influences the adsorption of MG, BBE133, and NR in single, binary and ternary systems. The MG+NR system exhibit maximum adsorption at approximately pH 10, while MG and MG+BBE133 systems showed peak adsorption around pH 6 and 10. The ternary displayed relatively minor fluctuations across the investigated pH ranges. These variations may be attributed in changes in adsorbent surface charge, dyes ionization, and electrostatic interactions as well as competition adsorption site (Yagub *et al*., 2014; Dutta *et al*., 2021)

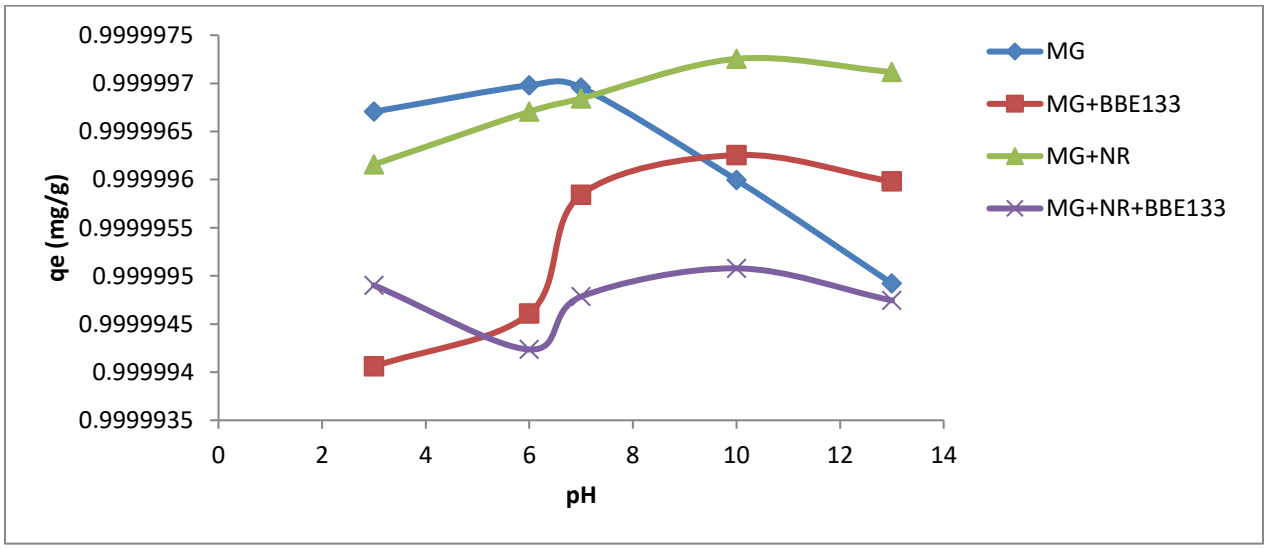


Fig. 10: Effect of pH

3.5.5 Effect of temperature

Fig. 11 illustrates the effect of temperature on the equilibrium adsorption capacity (qe) of the four systems. The adsorption capacity decreased with increasing temperature from 298 to 338 K, with the most pronounced decline observed for MG+BBE133, followed by MG+NR, MG+NR+BBE133, and MG. In contrast, MG exhibited relatively stable adsorption capacity across the investigated temperature range. These findings indicate that the temperature dependence of adsorption varies with system composition and suggest a possible reduction in adsorption favourability at elevated temperatures (Chen *et al*., 2012: Aumeier *et al*., 2022)

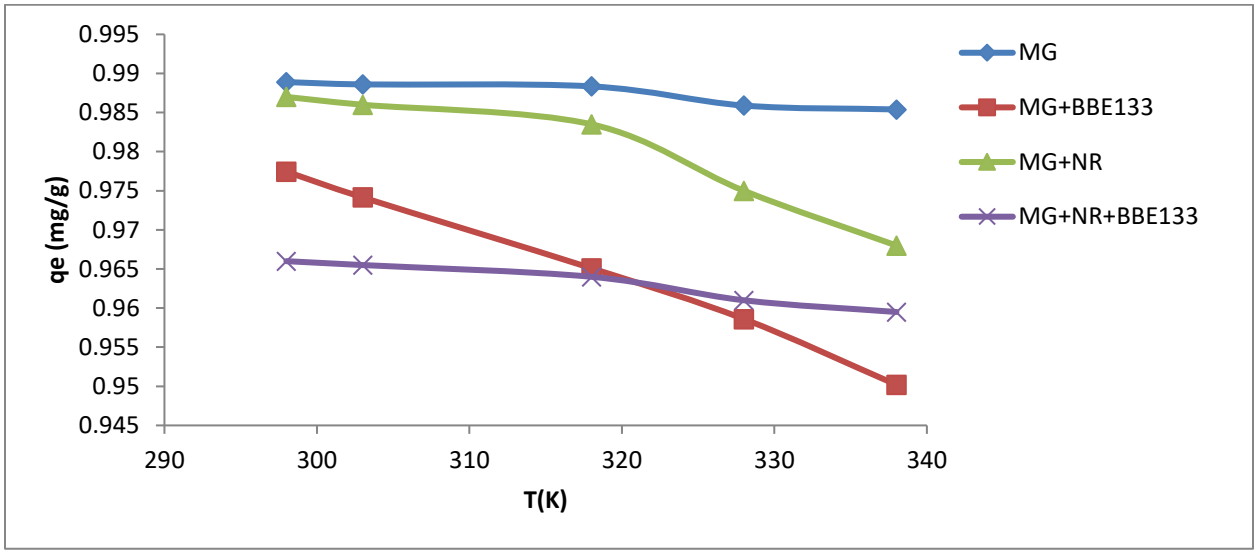


Fig. 11: Effect of Temperature

3.6 Kinetic study

The adsorption kinetics of dyes onto ACPMAC was evaluated using the pseudo-first-order, pseudo-second-order, intraparticle diffusion, and Elovich models. The pseudo-second-order model provided the best overall fit, with coefficients of determination (R^2) ranging from 0.9996 to 0.9997, accompanied by close agreement between experimental and calculated equilibrium adsorption capacities. In contrast, the pseudo-first-order and intraparticle diffusion models exhibited comparatively poor fits across most systems. The Elovich model also described the MG + BEE133 + NR system satisfactorily, yielding an R^2 value of 0.9961. These findings

indicate that the pseudo-second-order model most adequately represents the experimental adsorption kinetics under the investigated conditions. However, the excellent fit does not independently establish chemisorption as the rate-controlling mechanism, and further evaluation of mass-transfer effects and model residuals is required for mechanistic confirmation (Qiu *et al*., 2009; Plazinski *et al*., 2009; Simonin, 2016; Vareda, 2023).

Table 1: Kinetic Parameters for the Adsorption of dyes onto ACPMAC

Kinetic model	Parameters	MG	MG + BBE133	MG + NR	MG + BBE133 + NR
Pseudo first order	k_1	0.9760	0.0102	0.0306	0.0315
	$q_{e\ exp.}$	1.91	1.00	1.00	1.00
	$q_{e\ cal}$	2.0×10^{-3}	9.71×10^{-6}	1.85×10^{-6}	1.46×10^{-5}
	R^2	0.8794	0.5072	0.062	0.0454
Pseudo second order	k_2	2.363	7.024	14.13	1.736
	$q_{e\ exp.}$	1.991	1.000	1.000	1.000
	$q_{e\ cal}$	1.993	1.000	1.000	1.004
	R^2	0.9996	0.9996	0.9997	0.9996
Intra particle diffusion	K_{id}	1×10^{-5}	2×10^{-7}	8×10^{-8}	8×10^{-8}
	C	2.001	1.00	1.00	1.00
	R^2	0.6814	0.0919	0.0325	0.2677
Elovich	β	1×10^{5}	1×10^{6}	1.25×10^{5}	2×10^{5}
	R^2	0.6814	0.2387	0.3119	0.9961

3.7 Adsorption isotherm

The equilibrium adsorption data for dyes onto ACPMAC were analysed using the Langmuir, Freundlich, Temkin, Dubinin–Radushkevich, Harkins–Jura, Jovanovic, and Redlich–Peterson isotherm models. The results indicate that the suitability of each model varied across the investigated systems. The Langmuir model exhibited an excellent fit for MG, with an R^2 value of 0.9937, suggesting that monolayer adsorption may adequately describe this system. However, the Freundlich model provided a comparatively better fit for MG + BEE133 (R^2=0.9789),

whereas the Dubinin–Radushkevich model showed a high coefficient of determination for MG + NR (R^2=0.9629). For MG + BEE133 + NR, the Langmuir model yielded an R^2 value of 0.9418. Overall, the variation in model performance suggests that the adsorption behaviour depends on the composition of the dye system and may involve different surface interactions. Nevertheless, model selection should consider the complete set of fitted parameters and statistical errors rather than R^2 alone. Furthermore, the isotherm fits provide evidence of adsorption behaviour but do not independently establish the underlying molecular mechanism (Langmuir, 1918; Freundlich, 1906; Foo and Hameed, 2010).

Table 2: Isotherm Parameters for the Adsorption of dyes onto ACPMAC

Isotherm model	Parameters	MG	MG + BBE133	MG + NR	MG + BBE133 + NR
Langmuir	q_m (mg/g)	16.86	23.31	14.41	10.36
	K_L (L/mg)	0.285	0.543	0.208	0.107
	R_L	0.637	0.479	0.707	0.823
	R^2	0.9337	0.9789	0.9462	0.9418
Freundlich	K_F (mg/g)(L/mg)$^{1/n}$	479.1	143.8	389.6	1358.6
	n	0.9790	1.128	0.9984	0.899
	1/n	1.0214	0.8869	1.0016	1.1127
	R^2	0.9514	0.9321	0.9170	0.9158
Temkin	K_T(mg/g)	32126	145509.1	10070.9	86335.8
	b_T (kj/mol)	0.0610	0.0661	0.0593	0.0482
	B_T	40.51	36.987	41.797	51.355
	R^2	0.9956	0.7503	0.7391	0.9028
Dubinin Radushkevich	qm (mg/g)	4703.7	2239.7	3632.9	8145.3
	β (mol^2/J^2)	7.0×10^{-9}	7.0×10^{-9}	8.0×10^{-9}	1.0×10^{-8}
	E(Kj/mol)	8.451	8.452	7.906	7.071
	R^2	0.9285	0.9482	0.9314	0.9433
Hakin Jura	B	4.389	2.975	3.321	3.755
	A	3.026	4.677	4.177	3.894
	R^2	0.596	0.3241	0.3133	0.2917
Jovanovic	q_m (mg/g)	183.1	5154.8	7101.0	6575.8
	K_J	6.857	6.364	5.301	6.701
		0.571	0.6317	0.7083	0.6100

	R^2				
Redlich	β	0.9214	0.113	0.0523	0.2064
Peterson	A (L/g)	1486.6	143.77	652.8	4004.8
	R^2	0.8588	0.8825	0.0216	0.2291

3.8 Thermodynamics study

The thermodynamic parameters were evaluated to elucidate the temperature dependence and energetic characteristics of dye adsorption onto ACPMAC. The negative enthalpy changes (ΔH) reported for all systems indicate that the adsorption process is exothermic. The positive entropy changes (ΔS) suggest increased entropy at the solid–solution interface, potentially arising from changes in the arrangement of water molecules and adsorbed dye species. The negative Gibbs free energy changes (ΔG), as indicated by the table headings, suggest that adsorption is thermodynamically favourable over the investigated temperature range of 298–338 K. These findings are consistent with the established thermodynamic interpretation of adsorption processes (Foo & Hameed, 2010; Chen *et al*., 2021).

Table 3: Thermodynamics Parameter for the Adsorption of dyes onto ACPMAC

Adsorbates	-ΔH˚ (kj/mol)	ΔS˚ (J/k)	-ΔG˚(kj/mol)				
			298K	303K	318K	328K	338K
MG	16.87	37.03	27.94	28.05	28.63	29.04	29.38
MG+NR	19.12	34.79	29.33	29.63	30.66	30.46	30.68
MG+BBE133	31.62	5.93	29.74	29.63	30.66	29.07	29.62
MG+BBE133+NR	3.88	3.88	26.89	27.31	28.54	29.21	29.99

Conclusion

The adsorption of malachite green (MG) from single, binary and ternary dye systems onto ACPMAC was investigated. The optimal conditions for achieving maximum dye uptake were determined to be a pH range of 6–10, an adsorbent dosage of 0.1 g, a contact time of 15–105 min, and a temperature of 298 K. The adsorption kinetics was best described by the pseudo-second-order model. The equilibrium data were adequately fitted by the Langmuir, Freundlich,

and Dubinin–Radushkevich isotherm models, indicating that these models could effectively describe the adsorption process. Thermodynamic analysis revealed that the adsorption process was spontaneous and exothermic. In the binary dye system, the relative adsorption capacities indicated a synergistic interaction between the dyes during adsorption. Overall, the findings demonstrate that ACPMAC is a promising alternative adsorbent for the removal of cationic and anionic dyes from aqueous solutions.

Funding: This research received no external funding.

Acknowledgement: My special appreciation goes to my supervisor, Prof Abdulfatah Shehu Muhammad, my research team and the entire laboratory technologist of the Department of Pure and Industrial Chemistry, Bayero University Kano.

Conflict of Interest: The authors declare that there are no conflicts of interest.

Disclosure statement: Conflict of Interest: The authors declare that there are no conflicts of interest.

Compliance with Ethical Standards: This article does not contain any studies involving human or animal subjects.

Reference

Alias, S. S., Harun, Z., Azhar, F. H., Ibrahim, S. A., & Johar, B. (2019). Comparison between commercial and synthesised nano flower-like rutile TiO_2 immobilised on green super adsorbent towards dye wastewater treatment. *Journal of Cleaner Production, 251*, Article 119448.

Anyika, C., Asri, N. A. M., Majid, Z. A., Yahya, A., & Jafar, J. (2017). Synthesis and characterization of magnetic activated carbon developed from palm kernel shells. *Nanotechnology for Environmental Engineering, 2*, Article 16. https://doi.org/10.1007/s41204-017-0027

Arunprasath, T., Sudalai, S., Meenatchi, R., Jeyavishnu, K., & Arumugam, A. (2019). Biodegradation of triphenylmethane dye malachite green by a newly isolated fungus strain. *Biocatalysis and Agricultural Biotechnology, 17*, 672–679.

Aumeier, B. M., Augustin, A., Thönes, M., Sablotny, J., Wintgens, T., & Wessling, M. (2022). Linking the effect of temperature on adsorption from aqueous solution with solute dissociation. *Journal of Hazardous Materials, 429*, Article 128291. https://doi.org/10.1016/j.jhazmat.2022.128291

Bai, X., Yu, L., Hua, Z., Tang, Z., & Zhang, J. (2015). Synthesis and characterization of superparamagnetic activated carbon adsorbents based on cyanobacteria. *Materials Chemistry and Physics, 163*, 407–415.

Bai, Y., Chen, L., & Zhao, H. (2020). Adsorption behavior of synthetic dyes on magnetically modified adsorbents: SEM and FTIR characterization. *Journal of Hazardous Materials, 389*, Article 122102. https://doi.org/10.1016/j.jhazmat.2020.122102

Bhatti, H. N., Safa, Y., Yakout, S. M., Shair, O. H., Iqbal, M., & Nazir, A. (2020). Efficient removal of dyes using carboxymethyl cellulose/alginate/polyvinyl alcohol/rice husk composite: Adsorption/desorption, kinetics and recycling studies. *International Journal of Biological Macromolecules, 150*, 861–870.

Chen, T., Da, T., & Ma, Y. (2021). Reasonable calculation of the thermodynamic parameters from adsorption equilibrium constant. *Journal of Molecular Liquids, 322*, Article 114980. https://doi.org/10.1016/j.molliq.2020.114980.

Chen, Y., Liu, H., & Wang, J. (2020). Regeneration performance of magnetic activated carbon for dye adsorption: Mechanisms and limitations. *Journal of Environmental Chemical Engineering, 8*(5), Article 104112. https://doi.org/10.1016/j.jece.2020.104112

Chikri, R., Elhadiri, N., Benchanaa, M., & El Maguana, Y. (2020). Efficiency of sawdust as low-cost adsorbent for dyes removal. *Journal of Chemistry, 2020*, Article 8813420.

De Salomón, Y. L. O., Georgin, J., Franco, D. S. P., Netto, M. S., Foletto, E. L., Allasia, D., & Dotto, G. L. (2020). Application of seed residues from *Anadenanthera macrocarpa* and *Cedrela fissilis* as alternative adsorbents for remarkable removal of methylene blue dye in aqueous solutions. *Environmental Science and Pollution Research, 28*, 2342–2354.

Dotto, G. L., & McKay, G. (2020). Current scenario and challenges in adsorption for water treatment. *Journal of Environmental Chemical Engineering, 8*, Article 103988.

Dotto, J., Fagundes-Klen, M. R., Veit, M. T., Palácio, S. M., & Bergamasco, R. (2018). Performance of different coagulants in the coagulation/flocculation process of textile wastewater. *Journal of Cleaner Production, 208*, 656–665.

Dutta, S., Gupta, B., Srivastava, S. K., & Gupta, A. K. (2021). Recent advances on the removal of dyes from wastewater using various adsorbents: A critical review. *Materials Advances, 2*, 4497–4531. https://doi.org/10.1039/D1MA00354B

Du, Q., Zhang, S., Song, J., Zhao, Y., & Yang, F. (2020). Activation of porous magnetized biochar by artificial humic acid for effective removal of lead ions. *Journal of Hazardous Materials, 389*, Article 122115.

Enniya, I., Rghioui, L., & Jourani, A. (2018). Adsorption of hexavalent chromium in aqueous solution on activated carbon prepared from apple peels. *Sustainable Chemistry and Pharmacy, 7*, 9–16.

Feng, Z., Chen, H., Li, H., Yuan, R., Wang, F., Chen, Z., & Zhou, B. (2020). Preparation, characterization, and application of magnetic activated carbon for treatment of

biologically treated papermaking wastewater. *Science of the Total Environment, 713*, Article 136423.

Foo, K. Y., & Hameed, B. H. (2010). Insights into the modeling of adsorption isotherm systems. *Chemical Engineering Journal, 156*(1), 2–10. https://doi.org/10.1016/j.cej.2009.09.013

Freundlich, H. (1906). Über die Adsorption in Lösungen. *Zeitschrift für Physikalische Chemie, 57A*, 385–470.

Girish, C. R. (2025). Determination of thermodynamic parameters in adsorption studies: A review. *Chemical Papers, 79*, 5687–5706. https://doi.org/10.1007/s11696-025-04218-x

Grabi, M., Ahmed, S., & Khan, R. (2023). Surface morphology and adsorption efficiency of magnetically modified cellulose-based adsorbents. *Journal of Environmental Chemical Engineering, 11*(2), Article 109876. https://doi.org/10.1016/j.jece.2023.109876

Haleem, A., Shafiq, A., Chen, S.-Q., & Nazar, M. (2023). A comprehensive review on adsorption, photocatalytic and chemical degradation of dyes and nitro-compounds over different kinds of porous and composite materials. *Molecules, 28*, Article 1081.

Hassan, M. M., & Carr, C. M. (2018). A critical review on recent advancements of the removal of reactive dyes from dyehouse effluent by ion-exchange adsorbents. *Chemosphere, 209*, 201–219.

Husaini, M., Usman, B., & Ibrahim, M. B. (2024a). Biosorption of methyl orange dye in single, binary, and ternary systems onto gingerbread plum seed shell activated carbon. *Journal of the Turkish Chemical Society, 11*(2), 655–664. https://doi.org/10.18596/jotcs.1179829

Istratie, R., Stoia, M., Păcurariu, C., & Locovei, C. (2019). Single and simultaneous adsorption of methyl orange and phenol onto magnetic iron oxide/carbon nanocomposites. *Arabian Journal of Chemistry, 12*(8), 3704–3722. https://doi.org/10.1016/j.arabjc.2017.09.004

Jawad, A. H., Abdulhameed, A. S., Reghioua, A., & Yaseen, Z. M. (2020). Zwitterion composite chitosan-epichlorohydrin/zeolite for adsorption of methylene blue and reactive red 120 dyes. *International Journal of Biological Macromolecules, 163*, 756–765.

Kang, K., Nanda, S., Lam, S. S., Zhang, T., Huo, L., & Zhao, L. (2020). Enhanced fuel characteristics and physical chemistry of microwave hydrochar for sustainable fuel pellet production via co-densification. *Environmental Research, 186*, Article 109480.

Kumar, A., & Gupta, H. (2020). Activated carbon from sawdust for naphthalene removal from contaminated water. *Environmental Technology & Innovation, 20*, Article 101080.

Langmuir, I. (1918). The adsorption of gases on plane surfaces of glass, mica and platinum. *Journal of the American Chemical Society, 40*(9), 1361–1403. https://doi.org/10.1021/ja02242a004

Liu, X., Wang, Y., Zhang, T. C., Xiang, G., Wang, X., & Yuan, S. (2020). One-pot synthesis of a magnetic TiO_2/PTh/γ-Fe_2O_3 heterojunction nanocomposite for removing trace arsenite via simultaneous photocatalytic oxidation and adsorption. *Industrial & Engineering Chemistry Research, 60*, 528–540.

Mallakpour, S., Sirous, F., & Hussain, C. M. (2021). Sawdust, a versatile, inexpensive, readily available bio-waste: From mother earth to valuable materials for sustainable remediation technologies. *Advances in Colloid and Interface Science, 295*, Article 102492.

Moosavi, S., Lai, C. W., Gan, S., Zamiri, G., Pivehzhani, O. A., & Johan, M. R. (2020). Application of efficient magnetic particles and activated carbon for dye removal from wastewater. *ACS Omega, 5*, 20684–20697.

Noozi, B., & Social, G. A. (2013). Application models for multi-component adsorption site of dyes: A review. *Journal of Environmental Sciences, 25*(3), 419–429. https://doi.org/10.1016/S1001-0742(12)60194-6

Ortiz-Martínez, A., Godínez, L. A., Martínez-Sánchez, C., García-Espinoza, J., & Robles, I. (2021). Preparation of modified carbon paste electrodes from orange peel and used coffee ground. New materials for the treatment of dye-contaminated solutions using electro-Fenton processes. *Electrochimica Acta, 390*, Article 138861.

Patra, B. R., Mukherjee, A., Nanda, S., & Dalai, A. K. (2021). Biochar production, activation and adsorptive applications: A review. *Environmental Chemistry Letters, 19*, 2237–2259.

Pereira, D., Rocha, L. S., Gil, M. V., Otero, M., Silva, N. J. O., Esteves, V. I., & Calisto, V. (2020). In situ functionalization of a cellulosic-based activated carbon with magnetic iron oxides for the removal of carbamazepine from wastewater. *Environmental Science and Pollution Research, 28*, 18314–18327.

Plazinski, W., Rudzinski, W., & Plazinska, A. (2009). Theoretical models of sorption kinetics including a surface reaction mechanism: A review. *Advances in Colloid and Interface Science, 152*(1–2), 2–13. https://doi.org/10.1016/j.cis.2009.07.009

Puchana-Rosero, M., Adebayo, M. A., Lima, E. C., Machado, F. M., Thue, P. S., Vaghetti, J. C., Umpierres, C. S., & Gutterres, M. (2016). Microwave-assisted activated carbon obtained from the sludge of tannery-treatment effluent plant for removal of leather dyes. *Colloids and Surfaces A: Physicochemical and Engineering Aspects, 504*, 105–115.

Qiu, H., Lv, L., Pan, B.-C., Zhang, Q.-J., Zhang, W.-M., & Zhang, Q.-X. (2009). Critical review in adsorption kinetic models. *Journal of Zhejiang University-SCIENCE A, 10*, 716–724. https://doi.org/10.1631/jzus.A0820524

Rashid, J., Tehreem, F., Rehman, A., & Kumar, R. (2019). Synthesis using natural functionalization of activated carbon from pumpkin peels for decolourization of aqueous methylene blue. *Science of the Total Environment, 671*, 369–376.

Reza, R. A., & Ahmaruzzaman, M. (2015). A novel synthesis of Fe_2O_3@activated carbon composite and its exploitation for the elimination of carcinogenic textile dye from aqueous phase. *RSC Advances, 5*, 10575–10586. https://doi.org/10.1039/C4RA13601B

Sajjadi, S.-A., Meknati, A., Lima, E. C., Dotto, G. L., Mendoza-Castillo, D. I., Anastopoulos, I., Alakhras, F., Unuabonah, E. I., Singh, P., & Hosseini-Bandegharaei, A. (2019). A novel route for preparation of chemically activated carbon from pistachio wood for highly efficient Pb(II) sorption. *Journal of Environmental Management, 236*, 34–44.

Salem, S., Teimouri, Z., & Salem, A. (2020). Fabrication of magnetic activated carbon by carbothermal functionalization of agriculture waste via microwave-assisted technique for cationic dye adsorption. *Advanced Powder Technology, 31*, 4301– 4309.

Sarker, T. R., Pattnaik, F., Nanda, S., Dalai, A. K., Meda, V., & Naik, S. (2021). Hydrothermal pretreatment technologies for lignocellulosic biomass: A review of steam explosion and subcritical water hydrolysis. *Chemosphere, 284*, Article 131372.

Shah, L. A., Malik, T., Siddiq, M., Haleem, A., Sayed, M., & Naeem, A. (2019). TiO_2 nanotubes doped poly(vinylidene fluoride) polymer membranes (PVDF/TNT) for efficient photocatalytic degradation of brilliant green dye. *Journal of Environmental Chemical Engineering, 7*, Article 103291.

Shehu, A., & Muhammad, A. S. (2026). Adsorption of brilliant blue 133 dye in single, multicomponent system onto magnetic activated carbon as composite derived from *Ananas comosus* peels. *Journal of Applied Sciences and Environmental Studies, 9*(1), 81–94.

Simonin, J.-P. (2016). On the comparison of pseudo-first order and pseudo-second order rate laws in the modeling of adsorption kinetics. *Chemical Engineering Journal, 300*, 254–263. https://doi.org/10.1016/j.cej.2016.04.079

Supong, A., Bhomick, P. C., Baruah, M., Pongener, C., Sinha, U. B., & Sinha, D. (2019). Adsorptive removal of bisphenol A by biomass activated carbon and insights into the adsorption mechanism through density functional theory calculations. *Sustainable Chemistry and Pharmacy, 13*, Article 100159.

Tahir, M. A., Bhatti, H. N., & Iqbal, M. (2016). Solar Red and Brittle Blue direct dyes adsorption onto *Eucalyptus angophoroides* bark: Equilibrium, kinetics and thermodynamic studies. *Journal of Environmental Chemical Engineering, 4*, 2431–2439.

Thue, P. S., Umpierres, C. S., Lima, E. C., Lima, D. R., Machado, F. M., dos Reis, G. S., da Silva, R. S., Pavan, F. A., & Tran, H. N. (2020). Single-step pyrolysis for producing magnetic activated carbon from tucumã (*Astrocaryum aculeatum*) seed and

nickel(II) chloride and zinc(II) chloride. Application for removal of nicotinamide and propanolol. *Journal of Hazardous Materials, 398*, Article 122903.

Van Thuan, T., Quynh, B. T. P., Nguyen, T. D., Ho, V. T. T., & Bach, L. G. (2017). Response surface methodology approach for optimization of Cu^{2+}, Ni^{2+} and Pb^{2+} adsorption using KOH-activated carbon from banana peel. *Surfaces and Interfaces, 6*, 209– 217.

Vareda, J. P. (2023). On validity, physical meaning, mechanism insights and regression of adsorption kinetic models. *Journal of Molecular Liquids, 376*, Article 121416. https://doi.org/10.1016/j.molliq.2023.121416

Vieira, L. H. S., Sabino, C. M. S., Júnior, F. H. S., Rocha, J. S., Castro, M. O., Alencar, R. S., da Costa, L. S., Viana, B. C., de Paula, A. J., Soares, J. M., et al. (2020). Strategic design of magnetic carbonaceous nanocomposites and its application as multifunctional adsorbent. *Carbon, 161*, 758–771.

Wang, Y., Wang, S.-L., Xie, T., & Cao, J. (2020). Activated carbon derived from waste tangerine seed for the high-performance adsorption of carbamate pesticides from water and plant. *Bioresource Technology, 316*, Article 123929.

Wang, Y., Zhang, Y., Zhang, T. C., Xiang, G., Wang, X., & Yuan, S. (2020). Removal of trace arsenite through simultaneous photocatalytic oxidation and adsorption by magnetic Fe_3O_4@PpPDA@TiO_2 core–shell nanoparticles. *ACS Applied Nano Materials, 3*, 8495–8504.

Wekoye, J. N., Wanyonyi, W. C., Wangila, P. T., & Tonui, M. K. (2020). Kinetic and equilibrium studies of Congo red dye adsorption on cabbage waste powder. *Environmental Chemistry and Ecotoxicology, 2*, 24–31.

Yagub, M. T., Sen, T. K., Afroze, S., & Ang, H. M. (2014). Dye and its removal from aqueous solution by adsorption: A review. *Advances in Colloid and Interface Science, 209*, 172–184. https://doi.org/10.1016/j.cis.2014.04.002

Yunus, Z. M., Al-Gheethi, A., Othman, N., Hamdan, R., & Ruslan, N. N. (2019). Removal of heavy metals from mining effluents in tile and electroplating industries using honeydew peel activated carbon: A microstructure and techno-economic analysis. *Journal of Cleaner Production, 251*, Article 119738.

Zazycki, M. A., Godinho, M., Perondi, D., Foletto, E. L., Collazzo, G. C., & Dotto, G. L. (2018). New biochar from pecan nutshells as an alternative adsorbent for removing reactive red 141 from aqueous solutions. *Journal of Cleaner Production, 171*, 57–65.